ECOGRAPHY

Research

Size matters in quantitative radar monitoring of animal migration: estimating monitored volume from wingbeat frequency

Baptiste Schmid, Serge Zaugg, Stephen C. Votier, Jason W. Chapman, Mathieu Boos and Felix Liechti

B. Schmid (http://orcid.org/0000-0002-7736-7527) ✉ (baptiste.schmid@vogelwarte.ch) and F. Liechti (http://orcid.org/0000-0001-9473-0837), Swiss Ornithological Inst., Switzerland. – S. Zaugg, Swiss Birdradar Solutions, Switzerland, and Polytechnic Univ. of Catalonia, Laboratory of Applied Bioacoustics, Spain. – S. C. Votier (http://orcid.org/0000-0002-0976-0167) and J. W. Chapman (http://orcid.org/0000-0002-7475-4441), Centre for Ecology and Conservation, and Environment and Sustainability Inst., Univ. of Exeter, Penryn, Cornwall, UK. JWC also at: College of Plant Protection, Nanjing Agricultural Univ., Nanjing, China. – M. Boos, Research Agency in Applied Ecology, France.

Ecography
42: 931–941, 2019
doi: 10.1111/ecog.04025

Subject Editor: Cecilia Nilsson
Editor-in-Chief: Miguel Araújo
Accepted 28 December 2018

Quantitative radar studies are an important component of studying the movements of birds. Whether a bird, at a certain distance from the radar, is detected or not depends on its size. The volume monitored by the radar is therefore different for birds of different sizes. Consequently, an accurate quantification of bird movements recorded by small-scale radar requires an accurate determination of the monitored volume for the objects in question, although this has tended to be ignored.

Here, we demonstrate the importance of sensitivity settings for echo detection on the estimated movement intensities of birds of different sizes. The amount of energy reflected from a bird and detected by the radar receiver (echo power) depends not only on the bird's size and on the distance from the radar antenna, but also on the beam shape and the bird's position within this beam. We propose a method to estimate the size of a bird based on the wingbeat frequency, retrieved from the echo-signal, independent of the absolute echo power. The estimated bird-size allows calculation of size-specific monitored volumes, allowing accurate quantification of movement intensities. We further investigate the importance of applying size-specific monitored volumes to quantify avian movements instead of using echo counts.

We also highlight the importance of accounting for size-specific monitored volume of small scale radar systems, and the necessity of reporting technical information on radar parameters. Applying this framework will increase the quality and validity of quantitative radar monitoring.

Keywords: aeroecology, environmental impact assessment, radar

Introduction

The lowest two kilometres of the atmosphere host huge quantities of animal movements, often invisible to the human eye (Liechti and McGuire 2017, Reynolds et al. 2017), and there is an increasing interest to investigate the function and importance of the aerial habitat (Chilson et al. 2017, Bauer et al. 2019). There are several methods to monitor the movements of animals in the airspace (Drake and Bruderer 2017),

NORDIC SOCIETY OIKOS

www.ecography.org

with radar being the predominant technology when it comes to quantifying biomass flows (Chilson et al. 2017). Radar systems provide an ideal tool to monitor the temporal and spatial patterns of animal movements locally (Bruderer 1997, Fijn et al. 2015, Hu et al. 2016, Nilsson et al. 2018), as well as on a large scale (Gauthreaux et al. 2003, Chilson et al. 2012, Dokter et al. 2018, van Doren and Horton 2018, Nilsson et al. 2019). Therefore, the significance and demand for quantitative radar studies of animal movements in the context of ecological or environmental impact assessment studies has increased considerably (Bridge et al. 2011, Bauer and Hoye 2014, Bauer et al. 2017).

An accurate quantification of animal movements requires an adequate, but not easily accessible, knowledge of the monitored volume of the radar used (Schmaljohann et al. 2008, Drake and Reynolds 2012, Larkin and Diehl 2012). In principal, radars transmit electromagnetic waves that propagate in a three-dimensional beam along a main axis. The shape and extent of the beam defines the volume of air monitored by the radar. In addition to the characteristics of the radar system, the detection range, and thus, the monitored volume, depends strongly on the size of the object and its properties for reflecting the electromagnetic waves (Knott et al. 2004, Schmaljohann et al. 2008). Large objects are detected at farther distances and at wider angles from the beam axis than small ones (Fig. 1a). Because the energy density decays at a known rate with distance from the radar antenna (power law of four, see below Eq. 1), we can correct the echo power for its distance and estimate an object size defined by its reflective properties, its so-called radar cross section (RCS). This apparent RCS corrects for the distance along the main axis, but only refers to true RCS for objects that pass through the centre of the beam. Because the echo strength decreases with increasing angle from the beam axis, objects illuminated

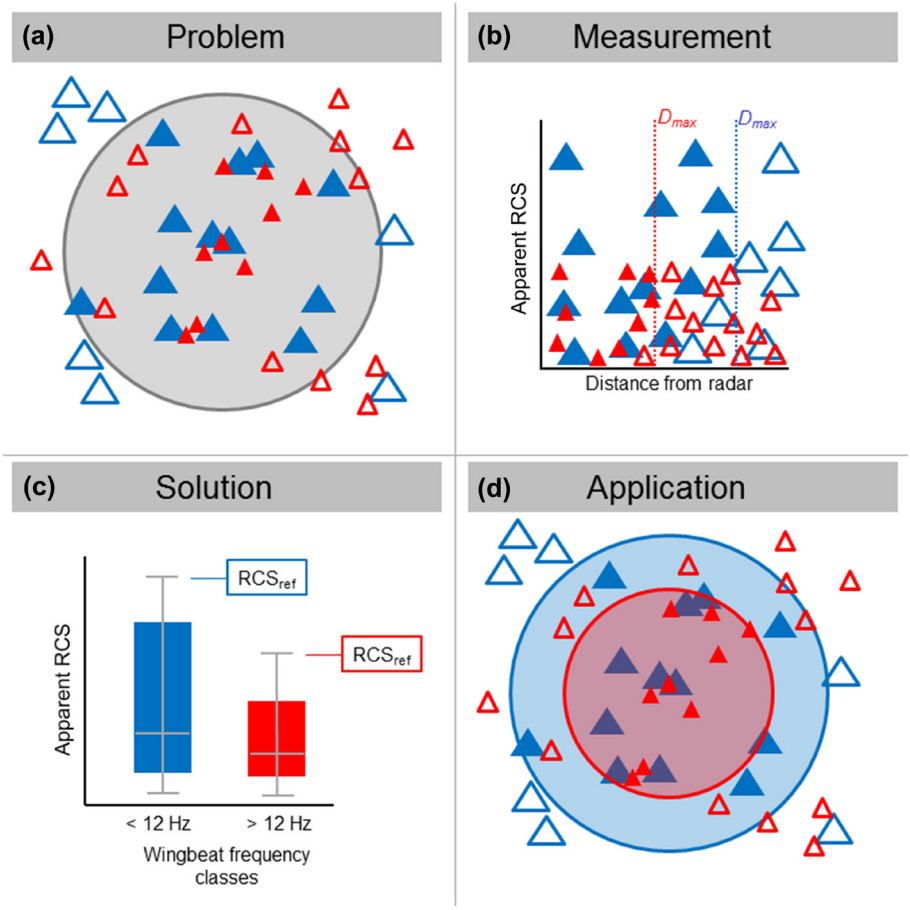

Figure 1. Research scheme. (a) Most radar studies assume a maximum detection distance (monitored volume, grey disk) for all detected objects (filled symbols), irrespective of their size (object size: blue > red). However, many small objects remain undetected (open symbols) within the maximum detection distance (red-open symbols within the grey circle). (b) Radars detect echoes with large RCS further away than echoes with small RCS (maximal detection distance D_{max} indicated by the vertical dotted line with the respective colour). Because the apparent RCS of objects decreases with increasing distance from the beam axis, the RCS of objects of different size overlap in the low ranges. Therefore, the actual size cannot be directly measured, but (c) the wingbeat frequency (WBF) can be used to separate large from small birds (Pennycuick 2001). The upper range of the RCS distributions should be closest to the true RCS due to individuals flying across the centre of the beam and serve as a reference RCS (RCS_{ref}) for object of similar size. (d) Applying RCS_{ref} results in size-specific detection monitored volume (blue and red disks).

in the periphery of the beam will appear smaller than an object of the same size detected in the beam centre (Fig. 1b). Therefore, the apparent RCS is a minimal measure of the true RCS, or the true object size, respectively. True RCS can hardly be measured directly by radar.

The frequency at which birds flap their wings is highly correlated with their body size, with larger birds flapping slower than small ones (Pennycuick 2001, Bruderer et al. 2010). This relationship has also been shown in several insect groups (Greenewalt 1962, Drake and Reynolds 2012). With respect to radar signals, the wingbeat frequency (WBF) of a bird can be estimated from the variation in echo intensity over time (echo signature) (Eastwood and Rider 1966, Bruderer and Joss 1969, Bruderer et al. 2010). Therefore, we can use the wingbeat frequency to estimate the size of the bird, independently from the apparent RCS (Fig. 1c). By assigning a given wingbeat frequency to a distinct RCS, we can estimate a bird-specific monitored volume (Fig. 1d).

In this study, we analysed six million echoes detected with a vertical-looking radar system (Nilsson et al. 2018), located at a range of sites along the African-Eurasian avian migratory flyway (from Sweden in the north, United Kingdom in the west, to Israel in the south-east), sampling birds from a wide geographic range. We used features of the echo signature to classify each echo into four echo-types ('passerine', 'wader', 'unidentified-bird', and 'non-bird'), and estimated the WBF (Zaugg et al. 2008). We first investigate how non-bird echoes, mainly insects, can be excluded from our sample by applying distance-dependent RCS-filters, and what the consequences are for the monitored volume. We then estimate the object sizes of birds with similar wingbeat patterns, and test whether the estimated object sizes are consistent across large geographical ranges that likely differ in the species composition of migratory birds. Finally, we highlight the importance of accounting for size-specific monitored volume in order to accurately quantify the height distributions of animal movements aloft. Our results highlight the importance of considering the size-specific monitored volume for each echo, and is an important step towards a more accurate quantitative estimate of animal movements using radar systems.

Methods

Radar physics in brief

Radar equation, RCS, and sensitivity filters

The radar equation describes the fundamental relationship of how the power registered by the receiver (P_r) can be determined as a function of the transmitted power (P_t), the distance (D) and the properties of the reflecting object (RCS). For point targets the radar equation can be formulated as follows (Drake and Reynolds 2012, Eq. 3.14a):

$$P_r = \frac{P_t \cdot G_0^2 \cdot \lambda^2 \cdot RCS}{(4 \cdot \pi)^3 \cdot D^4} \quad (1)$$

Apart from the wave-length (λ), the received power also depends on how the energy is distributed in space due to the characteristics of the antenna and how the energy reflected by an object is concentrated by the antenna. Thus, the shape of the antenna has a two-fold impact, which is defined as the antenna gain (G_0 [dB]). The received power P_r is the only object-specific quantity measured. We can rearrange the Eq. 1 to calculate a distance-corrected measure of the target size, the RCS (radar cross section) (Drake and Reynolds 2012, Eq. 4.1):

$$RCS = \frac{P_r \cdot (4 \cdot \pi)^3 \cdot D_{detect}^4}{P_t \cdot G_0^2 \cdot \lambda^2} \quad (2)$$

The minimal RCS (standing for 'object size') detectable at a given distance increases with the 4th power of the distance. As a consequence, the minimal RCS detectable at 10 m is 100 million times smaller than the one at 1 km. Hence, at close range a radar is much more sensitive than at farther distances. To exclude undesired echoes at short range, like reflections from ground (clutter), air turbulences or insects, most radar systems apply two different filters (Fig. 3a). A threshold based filter excludes all targets below a given received power P_r. Such a filter works independent of the distance and simply reduces the sensitivity of the radar system to exclude background noise in the system. A second, distance-dependent filter, named sensitivity time control (STC), supresses small targets at close range. The characteristics of an STC-filter can be defined by the distance at which a minimal RCS is still detectable, e.g. a 300 m STC-filter indicates that any object with an RCS only detectable up to 300 m will be excluded, while any larger object will be detected also within this distance.

Monitored volume and migratory traffic rates

Any quantitative monitoring is defined in time (duration) and space (detection range). The simplest non-directional antenna would propagate the same amount of energy in all directions and thus, the monitored volume would only depend on the reflecting properties of an object (RCS). However, almost all radars use antennas concentrating the emitted energy in a specific direction (Eastwood 1967, Drake and Reynolds 2012). The simplified radar equation presented in Eq. 1 describes the decay of the signal power along the beam axis. In order to estimate the monitored volume of a radar, it is further necessary to take into account for the decrease in echo power with increasing angle from the beam axis. The volume monitored for an object of given size (expressed as RCS) is defined by the maximum detection distance and the RCS specific beam angle (Fig. 2). Briefly, the radar equation (Eq. 1) can include the radar's beam pattern function $D(\theta)$ as follows:

$$P_r = \frac{\boldsymbol{D}(\theta) \cdot G_0^2 \cdot \lambda^2 \cdot RCS}{(4 \cdot \pi)^3 \cdot D^4} \quad (3)$$

We obtain the angular beam width θ_{thresh} [rad, °] using the inverse radar's beam pattern:

$$\theta_{thresh} = D^{-1\left(\frac{P_{r_{thresh}} \cdot (4 \cdot \pi)^3 \cdot D^2}{G_0^2 \cdot \lambda^2 \cdot RCS}\right)} \quad (4)$$

The angular beam width θ_{thresh} depends on the detection threshold $P_{r_{thresh}}$, the detection distance D and the RCS. Therefore, the volume monitored for an object of given RCS is defined by the maximum detection distance and the RCS specific angular beam width θ_{thresh}.

Migration traffic rate (MTR) is a standardised measure of bird movements that describes the number of birds crossing a virtual transect line of one kilometre within one hour (Lowery 1951, Liechti et al. 1995). The MTR therefore accounts for RCS and distance-dependent variation in monitored volume. For an object of a given RCS, we can estimate the width of the beam at its detection distance. The ratio between a one kilometre transect and the beam width serves as the correction factor to calculate MTR (hereafter referred as to MTR factor F_{MTR}):

$$F_{MTR} = \frac{1000}{Width_{beam}} \quad (5)$$

The MTR of a period between t_1 and t_2 is the sum of the MTR factors F_{MTR} multiplied by the ratio between an hour and the time period [hour] between t_1 and t_2:

$$MTR = \sum_{t_1 - t_2} F_{MTR} \cdot \frac{1}{t_1 - t_2} \quad (6)$$

Detailed calculations of the monitored volume are available in the appendix as an R-script (Supplementary material Appendix 5).

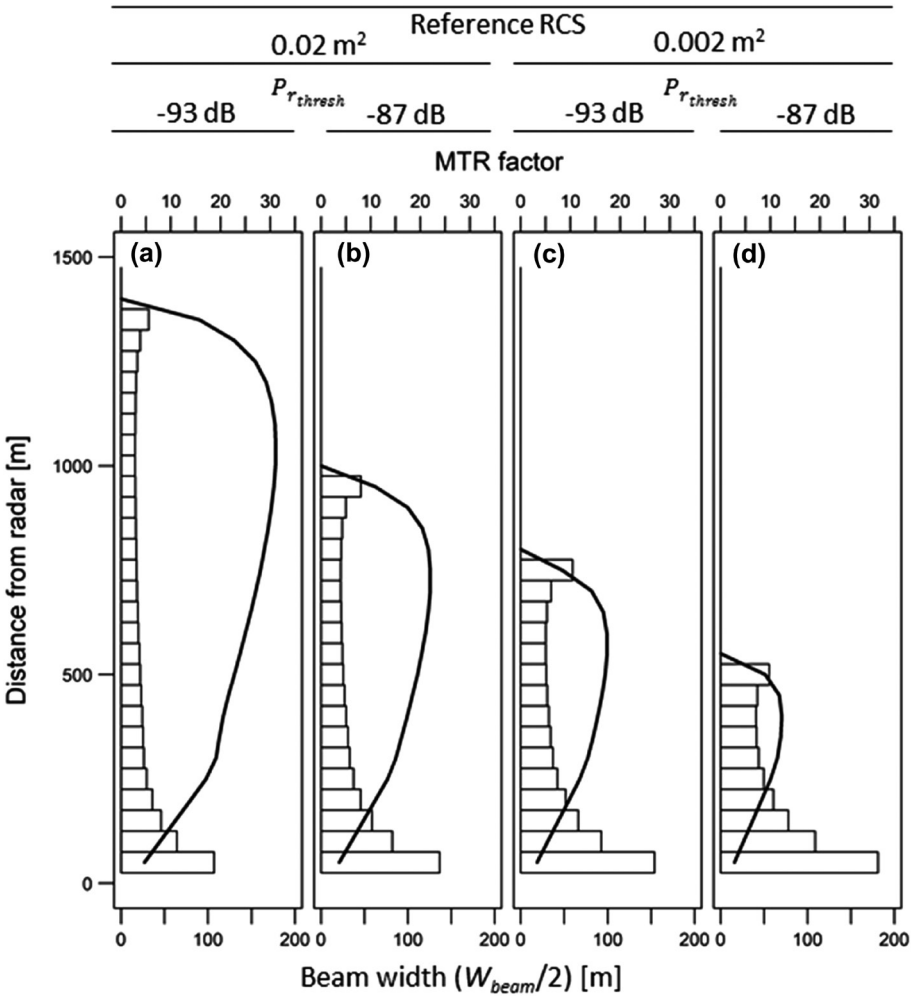

Figure 2. Beam width (solid lines, bottom x-axis) and MTR-factors (bars, 50 m distance bin, top x-axis) in relation to the distance for (a) –93 dB $P_{r_{thresh}}$ and 0.02 m² reference RCS, (b) –87 dB $P_{r_{thresh}}$ and 0.02 m² reference RCS, (c) –93 dB $P_{r_{thresh}}$ and 0.002 m² reference RCS, (d) –87 dB $P_{r_{thresh}}$ and 0.002 m² reference RCS. Further parameters to calculate the beam width: D_{STC} 300 m, P_t 20 kW, and waveguide attenuation 0 dB (see R-function in Supplementary material Appendix 5). Note the different scale of the x- and y-axes.

Echo detection, classification and wingbeat frequency

We used a modified X-band marine radar (Bridgemaster©, 25 kW, 9.4 GHz, wavelength ca 3.2 cm) with a vertical-looking 20 dB Horn antenna (17.5° nominal beam angle at –3 dB; Swiss BirdRadar Solution AG, swiss-birdradar.com). We used 70 ns short-pulse emission for a range resolution of 10 m and a maximal detection range of 1500 m. An automated software detects objects passing through the beam, and digitises the detected echo signals (sampling frequency = 425–450 Hz). The digitizer converts the received signal into dBm based on calibration measurements with a signal processing unit (Test Set 75, Gigaset) and a reference power of 1 mW. The echo signature describes the temporal variation of the echo power. The echo power is greatest when objects transit closest to the beam centre. The echo power also varies in relation to changes in the aspect of the object, such as the wingbeat movements of birds. To remove the small variations in echo intensity induced by changes in aspect, we apply a low pass filter (Chebyshev type I filters of order 5 with nominal band-pass limit set to 0.5 Hz) on the echo signature to identify the maximal echo power (hereafter referred to as echo power [dBm]). Because the intensity of the backscattered signal decays by distance at a known rate, we standardise the echo power with a distance correction given by the radar equation (Eq. 2).

This distance-corrected echo power is directly related to the RCS [m^2]. For a given object size, the RCS is maximal when the object passes through the beam axis, and minimal at the detection threshold at the periphery of the beam. We therefore referred to the measured RCS as apparent RCS. The echo power and its related RCS can strongly depend on the aspect of the animal in relation to the beam orientation (Edwards and Houghton 1959, Bruderer and Joss 1969, Mirkovic et al. 2016). Since vertical-looking radars illuminate animals from below ('ventral aspect'), the influence of aspect variation in a low-pass-filtered RCS is low and thus neglected in this study.

We used supervised learning to automate manual echo classification and manual assessment of wingbeat frequency (WBF). A band-pass filter (Chebyshev type I filters of order 5 with nominal band-pass limits set to 4 and 180 Hz) removed high frequency signal oscillations partly due to the 0.8 Hz rotation of the antenna. We used features derived from the echo signature (detailed features in Supplementary material Appendix 1 Table A1) and trained random forest classifiers to group the echoes into four echo-types ('passerine', 'wader', 'unidentified-bird', and 'non-bird'; Zaugg et al. 2008). Class probabilities are calculated for each echo, and the class with the highest probability is assigned to the echo. We re-classified echoes with class probabilities for passerine-type and wader-type lower than 0.5 as unidentified-bird-type. Non-bird echoes are insects and other non-determined objects. We assessed the WBF [Hz] with a random forest regression model trained with manually confirmed WBF values, and features extracted from band-pass echo signatures (detailed features in Supplementary material Appendix 1 Table A1). For each estimated WBF, a credibility factor is provided as the proportion of regression trees reaching close consensus. Cross validation of estimated WBF with manually determined WBF based on expert knowledge produced a Pearson correlation coefficient of 0.976 (on a subset of echoes with credibility factors ≥ 0.5). Because of the low-band pass filter, the trained classifier cannot determine WBF below 4 Hz. We restricted the WBF range to 25 Hz for birds (maximal known WBF for European birds, Bruderer et al. 2010) and to WBF with credibility factors larger than 0.5.

Data

We used data from 11 monitoring sites obtained during 2015–2017 (Table 1): Sempach (Switzerland (CH), year round), Col de Bretolet (CH, autumn), Geneva (CH, spring), Mölle (Sweden (SE), autumn), Sivry (France (FR), autumn), Herzeele (FR, autumn), Upper Galilee (Israel (IL), spring), Arava (IL, spring and autumn), Lower Galilee (IL, spring and autumn), Carmel (IL, spring and autumn), and Falmouth

Table 1. Overview of the 11 sites with radar monitoring: the geographic location (CH: Switzerland, SE: Sweden, FR: France, IL: Israel) and the monitoring period are provided, however the operation of the radar during these periods was not always continuous.

Site	Latitude, longitude	Altitude [m a.s.l.]	Start	End	Monitoring days (h)
Sempach (CH)	47.1, 8.2	450	Mar. 2016	Jun. 2017	504 (9707)
Geneva (CH)	46.2, 6.0	395	Mar. 2017	Jun. 2017	72 (1569)
Col de Bretolet (CH)	46.2, 6.8	1200	Aug. 2016	Oct. 2016	72 (1325)
Mölle (SE)	56.3, 12.5	70	Sep. 2015	Nov. 2015	62 (1384)
Herzeele (FR)	50.9, 2.5	10	Aug. 2016	Oct. 2016	59 (1124)
Sivry (FR)	48.8, 6.2	250	Oct. 2016	Nov. 2016	47 (967)
Upper Galilee (IL)	32.9, 35.2	350	Sep. 2015	Nov. 2015	66 (1417)
			Feb. 2016	May 2016	95 (2132)
Arava (IL)	30.7, 35.0	15	Mar. 2016	May 2016	81 (1911)
			Aug. 2016	Nov. 2016	79 (1795)
Lower Galilee (IL)	32.6, 35.4	115	Mar. 2016	Jun. 2016	77 (1799)
			Aug. 2016	Nov. 2016	92 (2168)
Carmel (IL)	32.6, 35.1	250	Aug. 2016	Nov. 2016	94 (2144)
Falmouth (UK)	50.2, –5.1	120	Mar. 2015	Mar. 2017	483 (5993)

(United Kingdom (UK), year round). During the course of these monitoring campaigns, the deployed radars registered 6 460 205 echoes, of which 660 200 were 'passerine-type' echoes (79.5% with WBF), 96 337 were 'wader-type' echoes (97.8% with WBF), 1 136 481 were 'unidentified-bird-type' echoes (44.1% with WBF), and 4 567 187 echoes were classified as 'non-bird-type'. This latter category undoubtedly consisted largely of insects, which at times can be hugely abundant in the atmosphere (Drake and Reynolds 2012, Hu et al. 2016). We also note that wader-type echoes may include echoes from bats (Bruderer and Popa-Lisseanu 2005). The WBF of bats range between 5 to 12 Hz (similar values to the bird species classified as wader-type), and bats follow similar WBF-body size relationship as birds (Bullen and McKencie 2002, Norberg and Norberg 2012). Further knowledge on cross-validated echo signatures may enable disentanglement of wader-type bird-echoes from bat-echoes. The monitoring campaigns differed in sensitivity settings: STC_{dist} ranged from 100 to 500 m, and detection threshold $P_{r_{min}}$ ranged from –100 to –90 dBm.

Analyses

Influence of sensitivity settings on monitored volume and on sample size

Radar users can adjust two detection sensitivity settings: the RCS-dependent filter (STC) and the detection threshold. We investigated how changes in these two sensitivity settings influence 1) the number of non-bird echoes, mainly insects, from the sampled data, and 2) the monitored volume. We used all echoes monitored with 300 m STC and –93 dBm detection threshold. We then applied post-hoc (after detection) the following sensitivity settings: STC 500 m, detection threshold –90, –87, and –83 dBm. In our study, a STC increase from 300 to 500 m increases the minimal RCS by a factor 7.7. An increase of three dB (a logarithmic scale) of the detection threshold corresponds to a two-fold increase in the required echoed energy for detection. We report changes in number of echoes detected for the following echo-types: passerine and non-bird.

We then illustrate the consequences of adjustable sensitivity settings (detection thresholds $P_{r_{thresh}}$: –93 dBm, –87 dBm) and reference RCS (0.002 or 0.02 m^2) on the monitored volume, especially on the maximum detection distance (D_{max}), and on MTR factors. Based on the radar equation, we estimate the monitored volume with an R-script (Supplementary material Appendix 5) and the following parameter: D_{STC} 300 m, P_t 20 kW, and waveguide attenuation 0 dB. We report the median of MTR-factors per 50 m distance bin.

Determination of reference RCS using wingbeat frequency

The only measure of the object size registered by radar is given by the apparent RCS, although the apparent RCS of objects decrease with the distance of the object from the beam axis (see above 'Radar physics in brief'). Because the estimation of the monitored volume requires knowledge of the object's RCS (Eq. 4), we form groups of birds of similar size using the echo type and the WBF to assign reference RCS to these birds. We use the distribution of the apparent RCS of all echoes per echo type and WBF interval to estimate a reference RCS. We report the 0.90- and 0.95-quantiles of the RCS distribution for each echo-type and 2-Hz WBF intervals. We used the results to estimate the MTR factors for each echo (see next section).

The species composition likely differs between the different geographical areas, and during spring and autumn migration events. We investigated whether the geographical region influences the observed RCS distributions. We used passerine-type echoes only because they are classified with high credibility, are abundant at each site and cover the entire range of WBF. We tested the dependency of the 0.9-quantile of the RCS (square-root transformed; using the 0.95-quantiles lead to similar results) on 2-Hz WBF interval (as ordered factors), adding the site identity as a random intercept in linear mixed-effects models as implemented in the 'lme4' R-package (Bates et al. 2015, R ver. 3.4.3), assuming a Gaussian distribution of the residuals.

Distance distribution corrected for size-specific monitored volume

To demonstrate the influence of MTR-factors on the estimate of migration intensity, we compared the distance distribution of the detected echoes with the distance distribution of MTR-factors. For each type of bird echo and WBF, we used the reference RCS determined by the 0.90-quantile distribution of RCS (analyses with the 0.95 quantile were quantitative similar). The calculation of MTR-factor for each echo is based on the radar equation (Eq. 1) and requires the following information: reference RCS (Supplementary material Appendix 2 Table A2), the distance (echoes are binned into 50 m distance intervals), the two sensitivity settings $P_{r_{thresh}}$ and D_{STC}, the transmitted power P_t specified by the radar type, and the radiation pattern as provided by the antenna manufacturer (Supplementary material Appendix 5, R-function 'funMTRfactor'). We calculated the MTR-factors for all bird echoes registered with maximum $P_{r_{thresh}}$ of –93 dBm and D_{STC} of 300 m, so that echo detection is based on a radar beam of the same shape.

Data deposition

Data available from the Zenodo Digital Repository: <https://zenodo.org/record/1311716> (Schmid et al. 2019).

Results

Influence of sensitivity settings on monitored volume and on sample size

An increase of the detection threshold by 6 dB reduced the effective beam area (planar projection of the monitored volume along the distance axis) by about 50% (Fig. 2: $P_{r_{thresh}}$ –93 dBm vs –87 dBm, see also Supplementary material Appendix 3

Table 2. Influence of sensitivity settings (D_{STC} and $P_{r_{thresh}}$) on the minimal RCS for detection RCS_{min}, the number of echoes, and the proportion of passerine-type and non-bird-type echoes. The total number of echoes also include wader-type and unidentified-bird-type echoes.

				Proportion of echoes	
D_{STC} [m]	$P_{r_{thresh}}$ [dBm]	RCS_{min} [m²]*	No. echoes	Passerine	Non-bird (insect)
300	–93	$3.6\ 10^{-5}$	2915284	0.181	0.589
300	–90	$7.2\ 10^{-5}$	1330121	0.279	0.423
300	–87	$1.4\ 10^{-4}$	664900	0.381	0.224
300	–83	$3.6\ 10^{-4}$	282270	0.418	0.064
500	–93	$2.7\ 10^{-4}$	1108448	0.342	0.171
500	–90	$5.5\ 10^{-4}$	455769	0.369	0.047
500	–87	$1.1\ 10^{-3}$	193102	0.265	0.020
500	–83	$2.7\ 10^{-3}$	52868	0.085	0.015

*using antenna gain G_0=20 dB; transmitted power $P_{t,W}$=20 kW.

Table A3). In particular, the maximal detection distance D_{max} decreased from 1361 m ($P_{r_{thresh}}$ –93 dBm) to 949 m ($P_{r_{thresh}}$ –87 dBm) for objects of 0.02 cm² reference RCS, and from 765 m ($P_{r_{thresh}}$ –93 dBm) to 527 m ($P_{r_{thresh}}$ –87 dBm) for objects of 0.002 cm² reference RCS (Supplementary material Appendix 3 Table A3, Fig. 2). In contrast, an increase of D_{STC} from 300 to 500 m had only a minor effect on the beam area (< 10%, Table 3) and does not affect the maximum detection distance as long as the object is large enough to be detected within the STC range.

The MTR-factors are inversely proportional to the beam width. Setting higher detection threshold $P_{r_{thresh}}$ reduces the maximal detection distance D_{max}, and the MTR-factors above D_{max} are undefined and set equal to zero. Within D_{max}, setting a higher detection threshold or STC reduces the beam width, therefore increasing the MTR-factors at a given height. Similarly, at a given height, the MTR-factors of large objects are smaller than the MTR-factors of small objects.

An increase of the detection threshold and STC lowers the measurement sensitivity and reduces the number of detected echoes (Table 2, Fig. 3). Obviously, a reduction of the sensitivity increases RCS_{min} (Table 2). By increasing the STC, small objects, especially echoes classified as non-bird type (Fig. 3), are reduced considerably. The proportion of non-bird echoes decreases from 59% (Table 2: STC_{dist} 300 m, $P_{r_{min}}$ –93 dBm) to less than 20% of the detected echoes (Table 2: STC_{dist} 500 m, $P_{r_{min}}$ –93 dBm). This 200 m increase of STC excluded 89% of the non-bird echoes, but only 28% of the passerines-type echoes. Increasing the detection threshold not only excludes small objects, it also reduces the monitored volume for any given object size. An increase in the detection threshold (–93 to –90 dBm; Table 2) decreases the proportion of non-bird echoes to 42% by excluding 67% of theses echoes, but this also leads to an exclusion of 30% of the passerine-type echoes.

Determination of reference RCS using wingbeat frequency

The apparent RCS decreased with increasing WBF for all three types of bird echoes (Fig. 4). Considering echoes with similar WBF, the median RCS is smallest for passerine-type, generally highest for wader-type, whereas unidentified birds tend to show intermediate median values. The 0.90-quantile distributions of apparent RCS parallel the 0.95-quantile distributions. We hereafter denominate the 0.90-quantile as the reference RCS, and we report the square-root of the reference RCS, since it approximates the size of birds at a tangible scale.

Wader-type echoes with low WBF (4–10 Hz) typically had reference RCS of 10–13 cm. The wader-type echoes with 11 ± 1 Hz WBF had a smaller reference RCS than echoes with 13 ± 1 Hz WBF (Fig. 4). The relatively few wader-type echoes with WBF larger than 13 Hz only occurred in non-rotation mode and mostly occurred during night time. Passerine-type echoes with low WBF (4–12 Hz) had reference

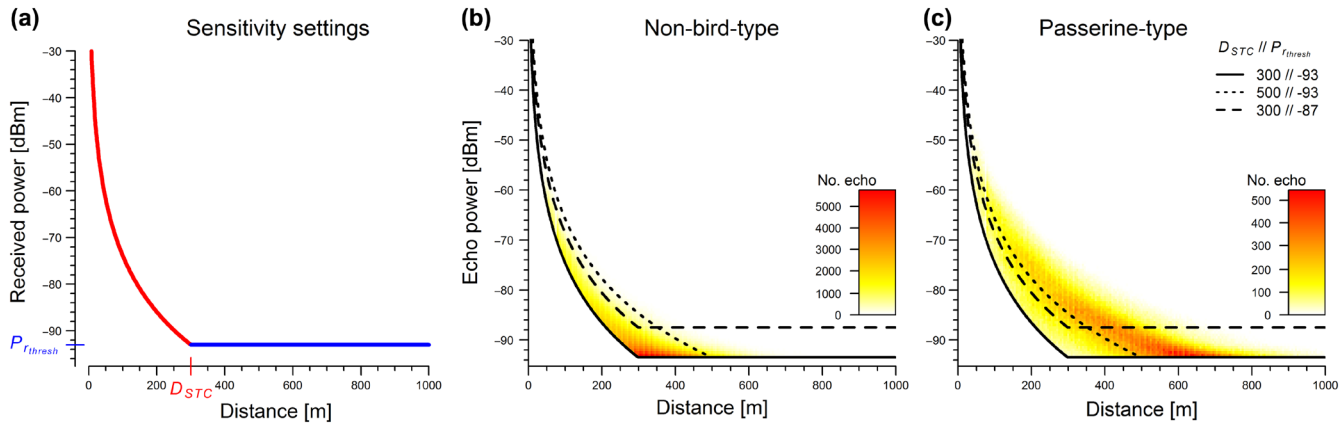

Figure 3. Distance dependence of (a) received power thresholds set by RCS-dependent (also referred as to STC-filer, red) and detection threshold (blue), (b) echo power for non-bird-type echoes (mostly 'insect'), and (c) echo power for passerine-type echoes. Lines delimit distance dependent detection thresholds: 1) D_{STC} 300 m and $P_{r_{thresh}}$ –93 dBm (solid line), 2) D_{STC} 500 m and $P_{r_{thresh}}$ –93 dBm (dotted line), and 3) D_{STC} 300 m and $P_{r_{thresh}}$ –87 dBm (dashed line). Note the different scale of the number of echo between non-bird-type and passerine-type echoes.

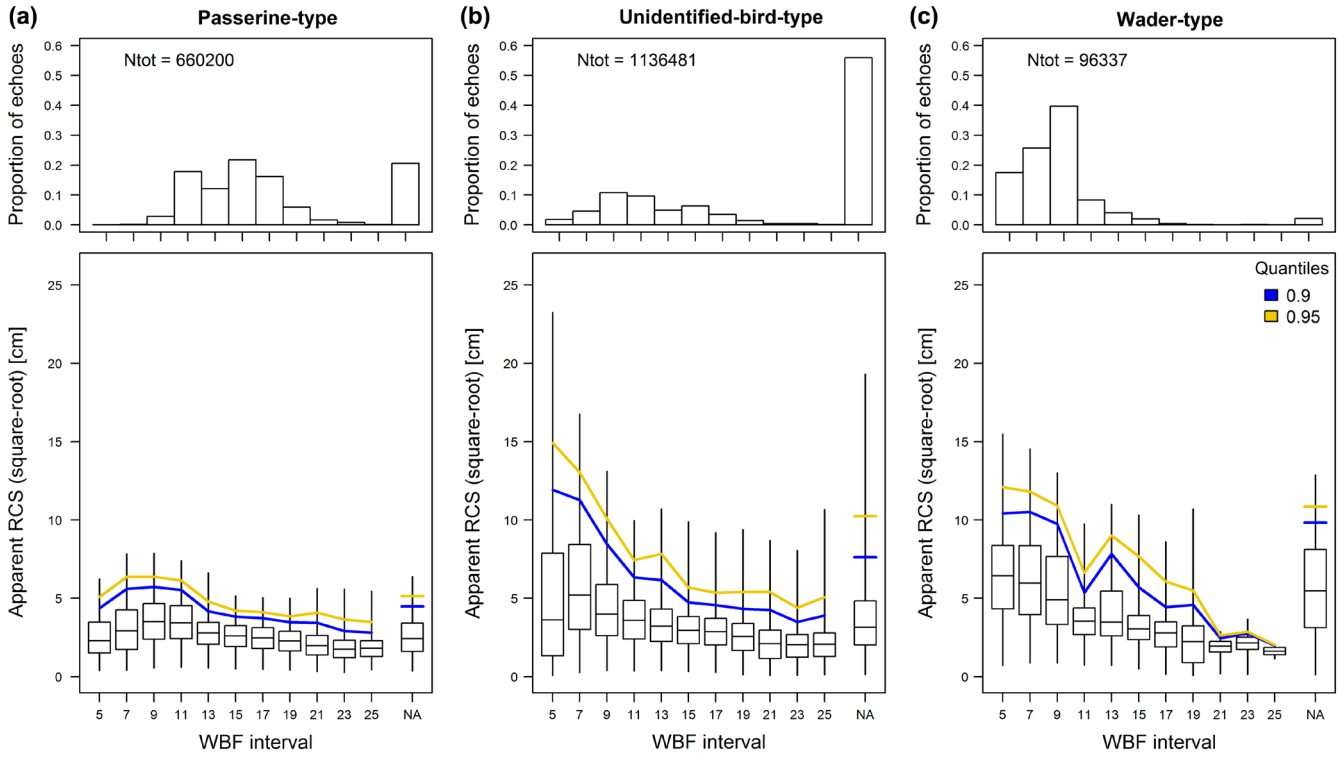

Figure 4. Distributions of apparent RCS per 2 Hz WBF intervals for echoes of (a) passerine-type, (b) unidentified-bird-type, and (c) wader type. Boxes show the 0.25 and 0.75 quantiles (vertical lines are the 0.01 and 0.99 quantiles). Coloured lines indicate the 0.9 (blue) and 0.95 (yellow) quantile of the distributions of the apparent RCS per WBF-interval. Sample size (proportion of echo) indicated on top panels.

RCS of 6–7 cm. We observed a marked decrease in reference RCS between 11 Hz and 13 Hz WBF intervals. The reference RCS of passerines with WBF > 12 Hz decreased steadily to a minimal square-root value of 3.5 cm. Unidentified-bird-type echoes showed a steeper decrease in reference RCS between 5 and 13 Hz WBF intervals than between 13 and 25 Hz WBF intervals.

The reference RCS per 2 Hz WBF intervals for passerine-type echoes showed no differences between study sites (using the 0.95 RCS quantiles led to similar results). Between-site variance (0.17 ± 0.65) is about 20 times smaller than the averaged site value (Intercept 4.06 ± 0.07) and 10 times smaller than the decrease in RCS per two-Hertz (–2.08 ± 0.16; see also Supplementary material Appendix 4 Fig. A3).

Distance distribution corrected for object-size dependent beam width

For each bird type and WBF interval we determined a reference RCS by the 0.90-quantile of the apparent RCS distribution (Fig. 4). We calculated the beam-width and monitored volume for each reference RCS values (Supplementary material Appendix 2 Table A2) in order to derive an MTR-factor for each echo. Weighing each echo by it's MTR-factor considerably increased the proportion of low-flying birds (Fig. 5). Fifty percent of the echoes were detected below the first 428 m (0.25-quantile: 266 m; 0.75-quantile: 597 m, Fig. 5a), whereas 50% of the MTR occurred within the first 306 m (0.25-quantile: 167 m; 0.75-quantile: 499 m, Fig. 5b). According to the reference RCS per taxa, D_{max} of large passerines (passerine-type with WBF < 12 Hz) is 858 m, and D_{max} of small passerine echoes (passerine-type with WBF > 12Hz) is 723 m (Fig. 5). Beyond 723 m, the MTR-factors of passerine-type echoes with WBF > 12 HZ equals zero, and therefore beyond this limit movements of small-passerine were ignored.

Discussion

Inexperienced researchers using radar systems to quantify bird movements often assume that the coverage of a radar is related to the distance at which some birds can still be detected. This study provides a framework for the accurate quantification of avian movements with radar, taking into account the size-specific monitored volume. Using data collected from distinct areas across Europe, and a broad variety of flying animals, we estimated the size of a bird based on the WBF, independent of the echo power.

Influence of sensitivity settings

In this study, we assess the effects of adjustable sensitivity settings on the detection of echoes of diverse types. Increasing the STC effectively removes the numerous non-bird echoes of little power (2/3 of all detected echoes). A small probability

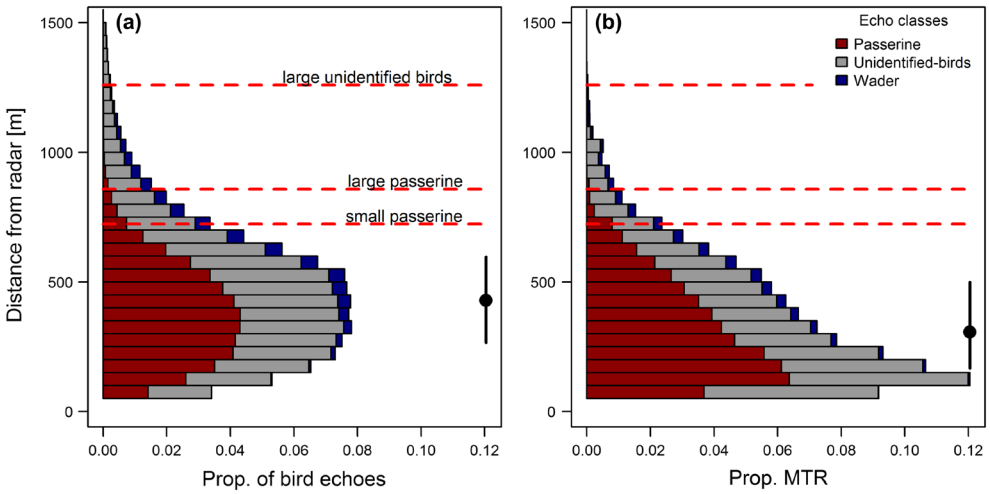

Figure 5. Distance distributions of (a) echoes and (b) MTR. Colours indicate echoes of different echo-types: red for passerine-type, grey for unidentified-bird-type, and blue for wader-type. The vertical black lines indicate the 0.25- and 0.75-quantiles, the dots indicate the median of the distance distributions. The horizontal red dashed lines indicate the maximal detection distances D_{max} ($P_{r_{thresh}}$ = –93 dBm, P_t = 20 kW, waveguide attenuation = 0 dB) for small passerine type (square-root reference RCS = 4.2 cm), large passerine type (square-root reference RCS = 5.7 cm), and large unidentified birds (square-root reference RCS = 11.9 cm). Above these lines, the MTR-factors equal zero for the respective echo groups.

of miss-classification of these non-bird echoes (insects) can produce high number of bird-type echoes, misleading subsequent analyses. The STC also has the advantage of acting only within the distance set by the STC, so it does not reduce the maximal detection distance of the target objects. In contrast, increasing the detection threshold significantly reduces the object-size specific monitored volume, in particular the maximal detection distance. Therefore, although a radar would detect large birds up to 2 km distances, the echoed power of smaller birds falls below the detection threshold at much smaller distances.

When possible, sensitivity settings should be selected to maximise echo detection. For a quantitative monitoring of avian migration, sensitivity settings (i.e. STC and detection threshold) should be appropriately selected in order to monitor movements of the smallest targeted bird taxa. Setting high STC values post-hoc can remove echoes from small birds in studies that focus on large birds only (e.g. geese). Therefore, adjusting the STC is an effective tool to match the specific aim and target object of radar monitoring. Furthermore, the appropriate radar parameters are required to correct for differences in the monitored volume.

Knowledge of radar parameters (wavelength, peak of transmitted power, antenna gain, waveguide attenuation, and the radiation pattern) and adjustable sensitivity settings (detection threshold and STC) are a prerequisite for any quantitative radar monitoring. Moreover, regular calibration will ensure registering of accurate information on standardised echo properties such as the echo power and its derived RCS (Atlas 2002, Schmaljohann et al. 2008, Drake and Reynolds 2012, May et al. 2017, Urmy and Warren 2017). Unfortunately, popular radar systems operating with built-in analysis software may not provide information on radar parameters and adjustable sensitivity settings to the end-users. In addition, some end-users can only monitor the radar display, not being able to register any quantitative information on the echo power (Nilsson et al. 2018). Such black-box radar systems render any quantitative assessment of animal movements difficult. As demonstrated in this study, the striking effects of adjustable sensitivity settings on the number of detected echoes per echo-type render the calibration and report of these sensitivity settings essential for any quantitative radar measurement.

Determination of reference RCS using WBF

We estimated the reference RCS from the echoed RCS for each echo-type (passerine-type, wader-type, and unidentified-bird-type) and WBF (2 Hz intervals). The smaller reference RCS of echoes with high WBF compared to echoes with lower WBF corroborate the negative correlation between body size and WBF defined in allometric flight models (Pennycuick 2001, Bruderer et al. 2010). The fact that the reference RCS are independent from the study site and season provides support to the general validity of using WBF to estimate the object size.

Using the 0.90- or 0.95-quantile of the RCS distributions provides bird size estimates close to experimental measurements of birds measured on the broad side (Edwards and Houghton 1959, Bruderer and Joss 1969, Vaughn 1985). Deviation from the relationship between the WBF and the related bird size can occur because of variation in flight behaviour. For instance, many passerine-type echoes with WBF lower than 8 Hz may originate from swallows performing flap-gliding flight instead of flap-bounding flight, resulting in WBF lower than expected (Rayner 1985, Liechti and

Bruderer 2002, Tobalske 2007). Passerines contribute to the large majority of inland avian migration fluxes (Hahn et al. 2009), and probably the majority of the unidentified-bird-type echoes are from passerine birds. Changes in the orientation of the bird's body within the beam can induce important changes in echo intensity, masking the regular modulation of the echo intensity due to the wingbeat patterns. Unidentified-bird-type echoes do not show a clear wingbeat type and less than 50% of the echoes had a credible WBF. Nevertheless, compared to passerine-type echoes, the upper RCS distribution of unidentified-bird-types is larger, probably because unidentified-bird-type echoes also include echoes from large soaring birds and bird flocks, shifting the RCS distributions to larger quantiles. Consequently, the over-estimation of the 0.90 RCS quantiles for unidentified-bird-type echoes leads to smaller MTR-factors, and an underestimation of the standardised movement intensity (MTR). The maximal WBF of wader-type birds reaches 12 Hz, with the notable exception of quails *Coturnix coturnix* (16 Hz, Bruderer et al. 2010), while some echoes with WBF > 12 Hz might be misclassifications.

The apparent RCS used in this study is not corrected for the decay in echo intensity with increasing distance from the beam axis. The rotation of the antenna on a slight nutated axis can allow the estimation of the angle between the entry- and exit-point of the object in the beam in relation to the beam centre. Assuming a straight flight, this angle can be used to calculate the closest distance between the object and the centre of the beam, and thus to correct the RCS accordingly (Drake and Reynolds 2012). This requires an accurate estimation of the beam width, and has not yet been implemented in the radar system used in this study. We here propose a method to determine the RCS according to the WBF, independently of the position of the object within the beam.

A similar approach could estimate the monitored volume for insects. Insects also show strong relationships between WBF and body size (Greenewalt 1962, Drake and Reynolds 2012). However, this relationship only holds within particular taxonomic groups, as insect taxa differ very much in size and wing shape. The estimation of insects' RCS based on WBF thus requires more detailed echo classification, or knowledge on flight phenology.

Distance distribution corrected for object-size dependent beam width

After correction for the monitored volume, the height (i.e. distance for a vertical looking antenna) distribution of the migration intensity is lower than if only reporting the height distribution of detected echoes. The differences in the height distribution of echoes and MTR highlight the potential misleading evaluation of collision risks of animals with human made structures such as wind turbines, bridges or power lines. In that regard, it is crucial that impact assessment studies accurately quantify the intensity of animal movements.

This article quantifies the importance of reporting standardised movements such as MTR to avoid detection biases. Equally important is to report the maximal detection ranges (Fig. 5) because important migration intensity can occur at high altitude (reviewed by Bruderer and Peter 2017, Bruderer et al. 2018), far above the maximal detection range of a particular monitoring scheme. Quantitative information on high migration events can be retrieved using longer pulse emission, available in many small radar systems, that increase the maximal detection distance. Alternatively, the increasing availability of weather radar data can complement height distribution retrieved from small scale radar systems (Nilsson et al. 2018).

Conclusions

Radar systems are valuable tools for the monitoring of aerial animal movements, but the results may suffer from important biases when the registered data is not processed adequately. In line with recent publications which detail adequate procedures (Schmaljohann et al. 2008, Drake and Reynolds 2012, Larkin and Diehl 2012, May et al. 2017, Urmy and Warren 2017) we hope that this publication will help to improve the scientific quality of radar monitoring.

We demonstrate the importance of accurately quantifying animal movement intensities, in particular for impact assessment studies of human-made structures (Aschwanden et al. 2018), or more generally to ecological studies of bioflows (Hu et al. 2016, Dokter et al. 2018). Fixed-beam radar systems have the great advantage of being able to retrieve detailed information on the registered echoes, such as the WBF. We show how the WBF can be used as an independent measure of the body size of the animal, and how this taxa-specific RCS provides the most accurate estimation of the monitored volume. When information on WBF is missing, citizen science data or expert knowledge on the body size of the birds involved in the investigated movements can allow the estimation of the monitored volume. Together with specific information on radar parameters (transmitted power, antenna gain, wavelength, radiation pattern) and sensitivity parameters (detection threshold, STC), information on the taxa specific RCS are essential for any quantitative monitoring of animal movement and should always be made available and reported.

Acknowledgements – This study was only possible thanks to the support of Daniel Früh, Dominik Kleger, Herbert Stark, Thomas Steuri, and Gregory Wills. We thank Cecilia Nilsson and two anonymous reviewers for their insightful comments that helped to further improve the quality of this article.
Funding – We acknowledge the financial support of COST – European Cooperation in Science and Technology – through the Action ES1305 'European Network for the Radar Surveillance of Animal Movement' (ENRAM) for facilitating international collaboration.
Author contributions – BS and FL conceived the study. BS, MB, SCV, JWC collected the data. BS, FL, SZ conducted the analyses. BS wrote the manuscript with substantial contributions from all authors.

References

Aschwanden, J. et al. 2018. Bird collisions at wind turbines in a mountainous area related to bird movement intensities measured by radar. – Biol. Conserv. 220: 228–236.

Atlas, D. 2002. Radar calibration: some simple approaches. – Bull. Am. Meteorol. Soc. 83: 1313–1316.

Bates, D. et al. 2015. lme4: linear mixed-effects models using Eigen and S4. – R package ver. 1.1-7.

Bauer, S. and Hoye, B. J. 2014. Migratory animals couple biodiversity and ecosystem functioning worldwide. – Science 344: 1242552.

Bauer, S. et al. 2017. From agricultural benefits to aviation safety: realizing the potential of continent-wide radar networks. – BioScience 67: 912–918.

Bauer, S. et al. 2019. The grand challenges of migration ecology that radar aeroecology can help answer. – Ecography 42: 861–875.

Bridge, E. S. et al. 2011. Technology on the move: recent and forthcoming innovations for tracking migratory birds. – BioScience 61: 689–698.

Bruderer, B. 1997. The study of bird migration by radar. Part 1: the technical basis. – Naturwissenschaften 84: 1–8.

Bruderer, B. and Joss, J. 1969. Methoden und Probleme der Bestimmung von Radarquerschnitten freifliegender Vögel. – Rev. Suisse Zool. 76: 1106–1118.

Bruderer, B. and Popa-Lisseanu, A. G. 2005. Radar data on wingbeat frequencies and flight speeds of two bat species. – Acta Chiropterol. 7: 73–82.

Bruderer, B. and Peter, D. 2017. Windprofit favouring extreme altitudes of bird migration. – Ornithol. Beob. 114: 73–86.

Bruderer, B. et al. 2010. Wing-beat characteristics of birds recorded with tracking radar and cine camera. – Ibis 152: 272–291.

Bruderer, B. et al. 2018. Vertical distribution of bird migration between the Baltic Sea and the Sahara. – J. Ornithol. 41: 282.

Bullen, R. D. and McKencie, N. L. 2002. Scaling bat wingbeat frequency and amplitude. – J. Exp. Biol. 205: 2615–2626.

Chilson, P. B. et al. 2012. Radar aeroecology: exploring the movements of aerial fauna through radio-wave remote sensing. – Biol. Lett. 8: 698–701.

Chilson, P. B. et al. (eds) 2017. Aeroecology. – Springer.

Dokter, A. M. et al. 2018. Seasonal abundance and survival of North America's migratory avifauna determined by weather radar. – Nat. Ecol. Evol. 2: 1603–1609.

Drake, V. A. and Reynolds, D. R. 2012. Radar entomology. Observing insect flight and migration. – CABI.

Drake, V. A. and Bruderer, B. 2017. Aeroecological observation methods. – In: Chilson, P. B. et al. (eds), Aeroecology. Springer, pp. 201–237.

Eastwood, E. 1967. Radar ornithology. – Methuen.

Eastwood, E. and Rider, G. C. 1966. Grouping of nocturnal migrants. – Nature 211: 1143–1146.

Edwards, J. and Houghton, E. W. 1959. Radar echoing area polar diagrams of birds. – Nature 184: 1059.

Fijn, R. C. et al. 2015. Bird movements at rotor heights measured continuously with vertical radar at a Dutch offshore wind farm. – Ibis 157: 558–566.

Gauthreaux, S. A. et al. 2003. Using a network of WSR-88D weather surveillance radars to define patterns of bird migration at large spatial scales. – In: Berthold, P. et al. (eds), Avian migration. Springer, pp. 335–346.

Greenewalt, C. H. 1962. Dimensional relationships for flying animals. – Smithsonian Miscellaneous Collections 144.

Hahn, S. et al. 2009. The natural link between Europe and Africa – 2.1 billion birds on migration. – Oikos 118: 624–626.

Hu, G. et al. 2016. Mass seasonal bioflows of high-flying insect migrants. – Science 354: 1584–1587.

Knott, G. et al. 2004. Radar cross section, 2nd ed. – The Inst. of Engineering and Technology.

Larkin, R. P. and Diehl, R. H. 2012. Radar techniques for wildlife research. – In: Silvy Nova, J. (ed.), Techniques for wildlife manual. John Hopkins Univ. Press, pp. 319–335.

Liechti, F. and Bruderer, L. 2002. Wingbeat frequency of barn swallows and house martins: a comparison between free flight and wind tunnel experiments. – J. Exp. Biol. 205: 2461–2467.

Liechti, F. and McGuire, L. P. 2017. Facing the wind: the aeroecology of vertebrate migrants. – In: Chilson, P. B. et al. (eds), Aeroecology. Springer, pp. 179–198.

Liechti, F. et al. 1995. Quantification of nocturnal bird migration by moonwatching: comparison with radar and infrared observations. – J. Field Ornithol. 66: 457–468.

Lowery, G. H. 1951. A quantitative study of the nocturnal migration of birds. – Univ. Kansas Publ. Mus. Nat. Hist. 3: 361–472.

May, R. et al. 2017. Performance test and verification of an off-the-shelf automated avian radar tracking system. – Ecol. Evol. 7: 5930–5938.

Mirkovic, D. et al. 2016. Electromagnetic model reliably predicts radar scattering characteristics of airborne organisms. – Sci. Rep. 6: 35637.

Nilsson, C. et al. 2018. Field validation of radar systems for monitoring bird migration. – J. Appl. Ecol. 278: 3074.

Nilsson, C. et al. 2019. Revealing patterns of nocturnal migration using the European weather radar network. – Ecography 42: 876–886.

Norberg, U. M. L. and Norberg, R. Å. 2012. Scaling of wingbeat frequency with body mass in bats and limits to maximum bat size. – J. Exp. Biol. 215: 711.

Pennycuick, C. J. 2001. Speeds and wingbeat frequencies of migrating birds compared with calculated benchmarks. – J. Exp. Biol. 204: 3283–3294.

Rayner, J. M. V. 1985. Bounding and undulating flight in birds. – J. Theor. Biol. 117: 47–77.

Reynolds, D. R. et al. 2017. Riders on the wind: the aeroecology of insect migrants. – In: Chilson, P. B. et al. (eds), Aeroecology. Springer, pp. 145–178.

Schmaljohann, H. et al. 2008. Quantification of bird migration by radar – a detection probability problem. – Ibis 150: 342–355.

Schmid, B. et al. 2019. Data from: Size matters in quantitative radar monitoring of animal migration: estimating monitored volume from wingbeat frequency. – Zenodo Digital Repository, <https://zenodo.org/record/1311716>.

Tobalske, B. W. 2007. Biomechanics of bird flight. – J. Exp. Biol. 210: 3135–3146.

Urmy, S. S. and Warren, J. D. 2017. Quantitative ornithology with a commercial marine radar: standard-target calibration, target detection and tracking, and measurement of echoes from individuals and flocks. – Methods Ecol. Evol. 8: 860–869.

van Doren, B. M. and Horton, K. G. 2018. A continental system for forecasting bird migration. – Science 361: 1115–1118.

Vaughn, C. R. 1985. Birds and insects as radar targets: a review. – Proc. IEEE 73: 205–227.

Zaugg, S. et al. 2008. Automatic identification of bird targets with radar via patterns produced by wing flapping. – J. R. Soc. Interface 5: 1041–1053.

Supplementary material (Appendix ECOG-04025 at <www.ecography.org/appendix/ecog-04025>). Appendix 1–5.